Medicinal Chemistry Research (2019) 28:608–622
https://doi.org/10.1007/s00044-019-02323-7

MEDICINAL CHEMISTRY RESEARCH

ORIGINAL RESEARCH

Furanchalcone–biphenyl hybrids: synthesis, in silico studies, antitrypanosomal and cytotoxic activities

Elisa García[1] · Rodrigo Ochoa[2] · Isabel Vásquez[1] · Laura Conesa-Milián[3] · Miguel Carda[3] · Andrés Yepes[1] · Iván D. Vélez[2] · Sara M. Robledo[2] · Wilson Cardona-G[1]

Received: 20 November 2018 / Accepted: 22 February 2019 / Published online: 11 March 2019

Abstract

The synthesis, antitrypanosomal, and cytotoxic activities of 17 furanchalcone derivatives are described herein. The structure of the synthesized products was elucidated by a combination of spectrometric analyses. The synthesized compounds were evaluated against *Trypanosoma cruzi*, which is the pathogenic species to humans. Cytotoxicity was evaluated against human U-937 macrophages. Eleven compounds were active against amastigotes of *T. cruzi* with EC_{50} values lower than 40 µM. Hybrids **7b–7d** and **8a–8g** showed better activity than benznidazole. Structure activity relationship (SAR) showed that the presence of electron withdrawing groups, such as nitro or fluorine, increased the activity and that the degree of oxygenation is essential for activity. In addition, molecular docking was used to identify a possible protein target for the designed compounds. A spearman correlation of 0.608 between the predicted scores and the experimental data profile the enzyme cruzipain as a potential candidate. Finally, in silico ADMET studies of the arylfuranchalcones showed that these novel compounds have suitable drug-like properties, making them potentially promising agents for antichagasic therapy.

Keywords Chagas disease · *Trypanosoma cruzi* · Furanchalcone · Hybrids · In silico studies · Biphenyl

Introduction

Neglected tropical diseases (NTDs) are a diverse group of communicable diseases that prevail in tropical and subtropical conditions in 149 countries. These diseases affect more than one billion people worldwide. NTDs include, among others, Chagas disease (American trypanosomiasis). This is a disease caused by the protozoan parasite *Trypanosoma cruzi* (*T. cruzi*) (WHO 2018a, 2018b).

Chagas disease, also known as American trypanosomiasis, is a potentially life-threatening illness and an important public health problem in Latin America. This disease currently affects around 8 million people in 21 countries, and is spreading by human migration to a number of nonendemic regions. Approximately, 20–30% of the infected population will suffer irreversible cardiovascular, gastrointestinal, and/or neurological problems. The two registered drugs for Chagas disease treatment are Nifurtimox and Benznidazole (BNZ), which require prolonged treatment and have frequent side-effects that can lead to discontinuation of treatment (WHO 2018a, 2018b). Based on the above, there is a need to look for new drugs for these diseases in order to provide a shorter treatment course, with fewer side-effects, and also to devise pediatric formulations.

Chalcones are a major class of natural products often found in edible plants. They have received considerable attention due to their wide range of biological actions, attributed due to their small structures and Michael acceptor features, which allows them to be tolerant to many biomolecules and at the same time confers on them the

Supplementary information The online version of this article (https://doi.org/10.1007/s00044-019-02323-7) contains supplementary material, which is available to authorized users.

✉ Sara M. Robledo
sara.robledo@udea.edu.co

✉ Wilson Cardona-G
wilson.cardona1@udea.edu.co

[1] Química de Plantas Colombianas, Institute of Chemistry, Faculty of Exact and Natural Sciences, University of Antioquia-UdeA, Calle 70 No. 52-21, A.A 1226 Medellín, Colombia

[2] PECET-Medical Research Institute, Faculty of Medicine, University of Antioquia-UdeA. Calle 70, No. 52-21, A.A 1226 Medellín, Colombia

[3] Department of Inorganic and Organic Chemistry, Jaume I University, E-12071 Castellón, Spain

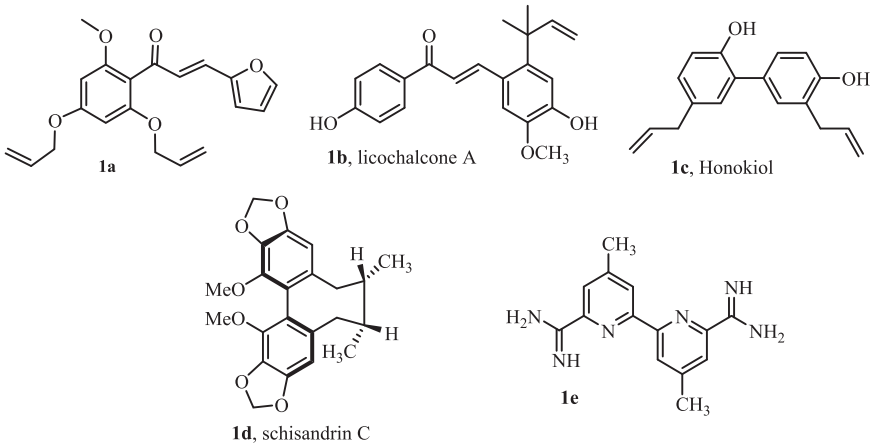

Fig. 1 Chalcones and biphenyls biologically actives

necessary reactivity to bind to their biological targets. For this reason, this class of compounds have been used as a scaffold in the development of different pharmacological agents (Singh et al. 2014; Zhuang et al. 2017; De Melo et al. 2018) including among them those endowed with antitrypanosomal activity (Bhambra et al. 2017). Some chalcones depicted in Fig. 1 show antiprotozoal activity, such as chalcone **1a**, which showed high trypanocidal activity against trypomastigotes of *T. cruzi* and low cytotoxicity (12.2 and 190.9 μM, respectively) with a selectivity index of 15.6 (Aponte et al. 2008) and licochalcone A (**1b**), an oxygenated chalcone isolated from the roots of *Glycyrrhiza* spp, a Chinese plant, which inhibited the fumarate reductase, a selective target present in the mitochondria of the parasite (Chen et al. 2001).

Many natural products, such as honokiol (**1c**) and schisandrin C (**1d**) (Fig. 1), exhibiting a biphenyl moiety in their structures are endowed with many relevant biological activities (Ma et al. 2011; Chen et al. 1997). In this regard, the biphenyl derivative **1e** (Fig. 1), whose structure is based on that of methylglyoxal bis(guanylhydrazone), was examined for in vitro antitrypanosomal activity and cytotoxicity on human cells. This compound had a half inhibitory concentration (IC_{50}) of 0.0041 μM against trypomastigotes form of *T. brucei rhodesiense*, and it was also active against other trypanosome species, including multidrug-resistant *T. b. brucei* ($IC_{50} = 0.29$, 0.005, and 0.012 μM against S427, K243, and K269 subgroup trypanosomes, respectively) (Brun et al. 1996).

A promising strategy based on hybrid molecules has recently emerged in medicinal chemistry for the discovery and development of new drugs. Hybrid molecules are chemical entities with two (or more than two) structural domains having different biological functions, and can therefore show a dual mode of action, acting as two distinct pharmacophores (Cardona-G et al. 2018; Meunier 2008) without necessarily acting on the same biological target (Shaveta and Singh 2016). In this sense we have synthesized several triclosan-caffeic acid hybrids and evaluated them against amastigotes of *T. cruzi*. Among the compounds tested, hybrids **2a** and **2b** exhibited the highest trypanocidal activity with a half effective concentration (EC_{50}) of 8.25 and 8.69 μM, respectively). These activities were even greater when compared against benznidazole, the reference drug ($EC_{50} = 40.3$ μM) (Otero et al. 2017). Triclosan and quinolone-hydrazone hybrids that were synthesized and evaluated in our group also exhibited good antitrypanosomal activity. Among these, hybrids **2c** and **2d** displayed the best results showing EC_{50} values of 1.10 and 4.6 μM, respectively (Vergara et al. 2017; Coa et al. 2015). Quinoline–chalcone hybrid **2e** also exhibited antitrypanosomal activity with a value of 31.73 μM (Coa et al. 2017). Furanchalcones–imidazole hybrids **2f** ($EC_{50} = 0.66$ μM) and **2g** ($EC_{50} = 0.72$ μM), furanchalcone–chromone hybrid **2h** ($EC_{50} = 13.78$ μM) and furanchalcone–quinoline hybrid **2i** ($EC_{50\text{-}T.cruzi} = 7.09$ μM) also exhibited a good activity against *T. cruzi* (García et al. 2018). Qiao et al. (2012) have also investigated the biological action of hybrid molecules such as chalcone–benzoxaborole hybrid **2j**, which showed an IC_{50} of 0.01 μg/mL against bloodstream form of *T. brucei* and elimination of parasitemia in a murine model of infection. On the other hand, M. A. Ismail and coworkers evaluated in vitro the biological action of biphenyl-benzimidazole-diamidines against *T. b. rhodesiense*, which showed IC_{50} values ranging from 3 to 37 nM, they found **2k** to be the most active compound with an IC_{50} value of 3.0 nM (Ismail et al. 2005) (Fig. 2).

In the search for new therapeutic alternatives to treat Chagas disease, a series of furanchalcone–biphenyl hybrids were designed, synthesized and evaluated in vitro in order to determine their cytotoxic and antitrypanosomal activities (Fig. 3). In addition, in silico studies were performed to associate a possible molecular target and predict drug-like properties.

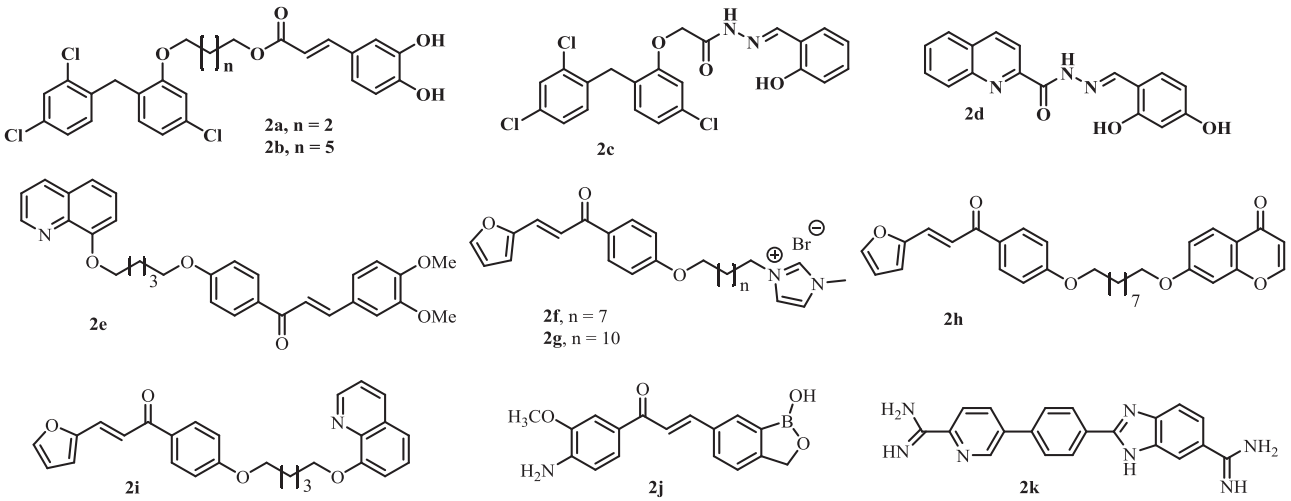

Fig. 2 Hybrid molecules derived from chalcone and biphenyl with antitrypanosomal activity

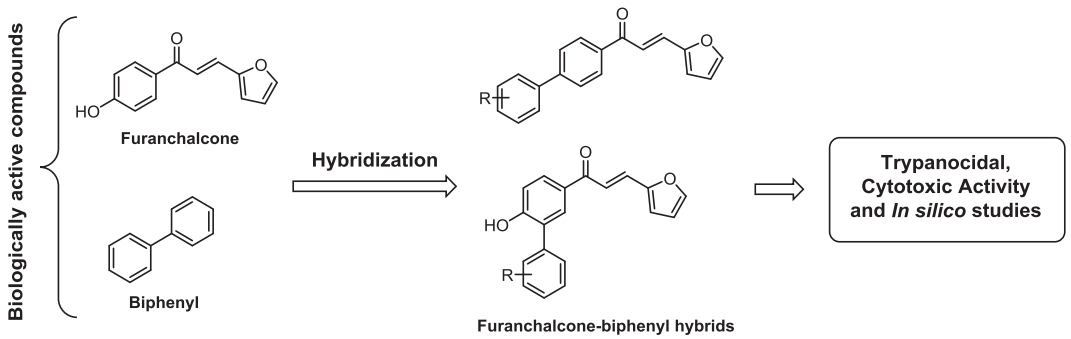

Fig. 3 Design of furanchalcone–biphenyl hybrids as antitrypanosomal agents

Material and methods

Chemical synthesis

General remarks

Microwave reactions were carried out in a CEM Discover microwave reactor in sealed vessels (monowave, maximum power 300 W, temperature control by IR sensor, fixed temperature). ^{1}H and ^{13}C nuclear magnetic resonance (NMR) spectra were recorded on a Varian instruments operating at 600 (300) and 150 (75) MHz, respectively. The signals of the deuterated solvent ($CDCl_3$ or CD_3OD) were used as reference ($CDCl_3$: $\delta = 7.27$ ppm for ^{1}H NMR and $\delta = 77.00$ ppm for ^{13}C NMR; CD_3OD: $\delta = 3.31$ and 4.87 ppm for ^{1}H NMR and $\delta = 49.2$ ppm for ^{13}C NMR). Carbon atom types (C, CH, CH_2, and CH_3) were determined by using the distortionless enhancement by polarization transfer or attached proton test pulse sequence. Signal, were assigned using two dimensional heteronuclear correlations (COSY, HSQC, and HMBC). High resolution mass spectra were recorded using electrospray ionization mass spectrometry (ESI-MS). A QTOF Premier instrument with an orthogonal Z-spray-electrospray interface (Waters, Manchester, UK) was used operating in the W-mode. The drying and cone gas was nitrogen set to flow rates of 300 and 30 L/h, respectively. Methanol sample solutions (ca. 1×10^{-5} M) were directly introduced into the ESI spectrometer at a flow rate of 10 µL/min. A capillary voltage of 3.5 kV was used in the positive scan mode, and the cone voltage set to Uc = 10 V. For accurate mass measurements, a 2 mg/L standard solution of leucine enkephalin was introduced via the lock spray needle at a cone voltage set to 85 V and a flow rate of 30 µL/min. IR spectra were recorded on a Spectrum RX I FT-IR system (Perkin-Elmer, Waltham, MA, USA) in KBr disks. Silica gel 60 (0.063–0.200 mesh, Merck, Whitehouse Station, NJ, USA) was used for column chromatography, and precoated silica gel plates (Merck 60 F254 0.2 mm) were used for thin layer chromatography (TLC).

General procedure for the synthesis of furanchalcones (4,5) Acetophenones **1** or **2** (1 eq) and furfural **3** (1.1 eq) were added to an ethanolic solution of NaOH 20%. The

mixture was sonicated for 45 min and neutralized with a solution HCl 10% in an ice bath. The resulting yellow solid was filtered, washed with water and dried. The solid was recrystallized with methanol to get the furanochalcones **4** and **5** with yields of 51% an 85%, respectively. Monitoring the reaction progress and product purification was carried by TLC.

***(2E)-3-(furan-2-yl)-1-(4-iodophenyl)prop-2-en-1-one (4)*:** Yield 51%; pale yellow solid; m.p. 61–64 °C; IR (cm^{-1}): ν_{max} 1658 (C = O), 1583 (C = C), 1543 (C = C_{Ar}), 995 (-C-O-C_{Furane}), 804 (C-H_{Ar}). ^{1}H-NMR ($CDCl_3$, 300 MHz): δ 6.57 (H_2, dd, *J1* = 1.70, *J2* = 3.23 Hz), 6.73 (H_3, d, *J* = 3.23 Hz), 7.38 (H_5, d, *J* = 15.32 Hz), 7.53 (H_1, $s_{apparent}$), 7.59 (H_6, d, *J* = 15.32 Hz), 7.73 (H_9, H_{10}, d, *J* = 8.45 Hz), 7.85 (H_{11}, H_{12}, d, *J* = 8.45 Hz); ^{13}C-NMR ($CDCl_3$, 75 MHz): δ 100.68 (C_{13}), 112.84 (C_2), 116.78 (C_3), 118.60 (C_6), 129.88 (C_9, C_{10}), 131.15 (C_5), 137.44 (C_8), 137.94 (C_{11}, C_{12}), 145.18 (C_1), 151.56 (C_4), 188.97 (C_7). ESI-MS: m/z 324.9725 $[M+H]^+$, Calc. for $C_{13}H_9IO_2$: 324.9726.

***(2E)-3-(furan-2-yl)-1-(4-hidroxy-3-iodophenyl)prop-2-en-1-one (5)*:** Yield 85%; yellow solid; m.p 169–170 °C; IR (cm^{-1}): ν_{max} 3369 (-OH), 1629 (C = O), 1579 (C = C), 1519 (C = C_{Ar}), 1014 (-C-O-C-$_{furane}$), 806 y 742 (C-H_{Ar}). ^{1}H-NMR (DMSO-d_6, 300 MHz): *δ* 6.68 (H_2, dd, *J1* = 1.8, *J2* = 3.5 Hz), 6.99 (H_{12}, d, *J* = 8.50 Hz), 7.09 (H_3, d, *J* = 3.5 Hz), 7.52 (H_5, H_1, $s_{apparent}$), 7.90 (H_6, s), 7.99 (H_9, dd, *J1* = 2.05, *J2* = 8.5 Hz), 8.38 (H_{10}, d, *J* = 2.05 Hz); ^{13}C-NMR (DMSO-d_6, 75 MHz): *δ* 85.63 (C_{11}), 113.55 (C_2), 115.10 (C_{12}), 117.14 (C_3), 118.89 (C_6), 130.40 (C_9), 131.14 (C_5), 131.19 (C_8), 140.10 (C_{10}), 146.52 (C_1), 151.69 (C_4), 161.62 (C_{13}), 186.01 (C_7). ESI-MS: *m/z* 294.9884 $[M+H]^+$, Calc. for $C_{13}H_9IO_3$: 294.9888.

General procedure for the synthesis of aryl-furanchalcones (7a–7i and 8a–8i): A mixture of 4-iodofuranochalcona **4** or 4-hydroxy-3-iodofuranochalcona **5** (1 eq), boronic acid **6a–i** (2 eq), palladium acetate (5%), triphenylphosphine (10%), sodium carbonate (7eq), and 4 mL of toluene:methanol (3:1), were heated under microwave radiation for 40 min (100 °C, 200 W). Then the mixture was diluted with dichloromethane and filtered. The crude reaction mixture was evaporated under reduced pressure and the residue was purified by preparative TLC eluting with a mixture of dichlorometahane:hexane (9:1). The final product was recrystallized to obtain the aryl-furanochalcones **7a–i** and **8a–i** with yield between 27–85% and 61–65%, respectively.

***(2E)-1-{2′,3′-dimethoxy-[1,1′-biphenyl]-4-yl}-3-(furan-2-yl) prop-2-en-1-one (7a)*:** Yield 35%; beige solid; m.p. 111–114 °C; IR (cm^{-1}): ν_{max} 2933 (-CH_3), 1666 (C = O), 1597 (C = C), 1548 (C = C_{Ar}), 1263 y 1035 (-OCH_3 $_{Ar}$), 1006 (-C-O-C- $_{furane}$), 796, 736 y 700 (C-H_{Ar}). ^{1}H-NMR ($CDCl_3$, 300 MHz): δ 3.60 (-O-C$\underline{H}_3$, s), 3.93 (-O-C$\underline{H}_3$, s), 6.53 (H_2, dd, *J*1 = 3.41 y *J2* = 1.80), 6.74 (H_3, d, *J* = 3.02 Hz), 6.93-7.02 (H_{15}, H_{17}, m), 7.15 (H_{16}, t, *J* = 7.88 Hz), 7.52 (H_1, H_6, d, *J* = 15.50 Hz), 7.63 (H_5, d, *J* = 15.50 Hz), 7.70 (H_{11}, H_{12}, d, *J* = 8.20 Hz), 8.09 (H_9, H_{10}, d, *J* = 8.20 Hz). ^{13}C-NMR ($CDCl_3$, 75 MHz): *δ* 56.00 (-O-C$\underline{H}_3$), 60.80 (-O-C$\underline{H}_3$), 112.24 (C_{17}), 112.71 (C_2), 116.25 (C_3), 119.38 (C_6), 122.40 (C_{15}), 124.31 (C_{16}), 128.36 (C_{11}, C_{12}), 129.59 (C_9, C_{10}), 130.59 (C_5), 134.88 (C_{14}), 136.77 (C_{14}), 142.94 (C_8), 144.94 (C_1), 146.65 (C_{19}), 151.78 (C_4), 153.23 (C_{18}), 189.54 (C_7). ESI-MS: *m/z* 335.1281 $[M+H]^+$, Calc. for $C_{21}H_{18}O_4$: 335.1283.

***(2E)-1-{2′,4′-dimethoxy-[1,1′-biphenyl]-4-yl}-3-(furan-2-iy) prop-2-en-1-one (7b)*:** Yield 34%; yellow pale solid; m.p. 114–117 °C; IR (cm^{-1}): ν_{max} 2927 (-CH_3), 1651 (C = O), 1583 (C = C), 1548 (C = C_{Ar}), 1211 y 1024 (-OCH_3 $_{Ar}$), 1004 (-C-O-C- $_{furane}$), 829, 759 y 677 (C-H_{Ar}). ^{1}H-NMR ($CDCl_3$, 300 MHz): *δ* 3.82 (-O-C$\underline{H}_3$, s), 3.86 (-O-C$\underline{H}_3$, s), 6.52 (H_2, dd, *J*1 = 1.80 y *J2* = 3.30 Hz), 6.55–6.63 (H_{16}, H_{18}, m), 6.72 (H_3, d, *J* = 3.30 Hz), 7.29 (H_{19}, d, *J* = 8.11 Hz), 7.51 (H_6, H_5, d, *J* = 14.99 Hz), 7.60 (H_1, $s_{apparent}$), 7.64 (H_{11}, H_{12}, d, *J* = 8.23 Hz), 8.07 (H_9, H_{10}, d, *J* = 8.23 Hz); ^{13}C-NMR ($CDCl_3$, 75 MHz): *δ* 55.50 (-O-$\underline{C}H_3$), 55.60 (-O-$\underline{C}H_3$), 99.07 (C_{16}), 104.90 (C_{18}), 112.69 (C_2), 116.09 (C_3), 119.46 (C_6), 122.38 (C_{19}), 128.30 (C_{11}, C_{12}), 129.61 (C_9, C_{10}), 130.40 (C_{14}), 131.35 (C_5), 136.06 (C_{13}), 143.24 (C_8), 144.86 (C_1), 151.83 (C_4), 157.64 (C_{15}), 161.00 (C_{17}), 189.39 (C_7). ESI-MS: *m/z* 335.1278 $[M+H]^+$, Calc. for $C_{21}H_{18}O_4$: 335.1283.

***(2E)-1-{2′,5′-dimethoxy-[1,1′-biphenyl]-4-yl}-3-(furan-2-yl) prop-2-en-1-one (7c)*:** Yield 47%; yellow pale solid; m.p. 87-90 °C; IR (cm^{-1}): ν_{max} 2935 (-CH_3), 1662 (C = O), 1604 (C = C), 1552 (C = C_{Ar}), 1220 y 1047 (-OCH_3 $_{Ar}$), 1016 (-C-O-C- $_{furane}$), 723 (C-H_{Ar}). ^{1}H-NMR ($CDCl_3$, 300 MHz): *δ* 3.77 (-O-C$\underline{H}_3$, s), 3.82 (-O-C$\underline{H}_3$, s), 6.52 (H_2, dd, *J*1 = 1.80 y *J2* = 3.41 Hz), 6.73 (H_3, d, *J* = 3.40 Hz), 6.83-6.98 (H_6, H_{17}, H_{18}, m), 7.51 (H_5, H_{15}, d, *J* = 15.66 Hz), 7.60 (H_1, s), 7.67 (H_{11}, H_{12}, d, *J* = 8.40 Hz), 8.08 (H_9, H_{10}, d, *J* = 8.4 Hz); ^{13}C-NMR ($CDCl_3$, 75 MHz): δ 55.87 (-O-$\underline{C}H_3$), 56.34 (-O-$\underline{C}H_3$), 112.71 (C_{18}), 112.79 (C_2), 113.94 (C_{17}), 116.21 (C_{15}), 116.62 (C_3), 119.40 (C_6), 128.29 (C_9, C_{10}), 129.76 (C_{11}, C_{12}), 130.49 (C_5), 130.57 (C_{14}), 136.66 (C_{13}), 143.13 (C_8), 144.92 (C_1), 150.82 (C_4), 151.79 (C_{19}), 153.84 (C_{16}), 189.46 (C_7). ESI-MS: *m/z* 335.1277 $[M+H]^+$, Calc. for $C_{21}H_{18}O_4$: 335.1283.

***(2E)-1-{2′,6′-dimethoxy-[1,1′-biphenyl]-4-yl}-3-(furan-2-yl) prop-2-en-1-one (7d)*:** Yield 46%; beige solid; m.p. 140–143 °C; IR (cm^{-1}): ν_{max} 2927 (-CH_3), 1652 (C = O), 1587 (C = C), 1550 (C = C_{Ar}), 1246 y 1103 (-OCH_3 $_{Ar}$), 1012

(-C-O-C- $_{furane}$), 732 (C-H_{Ar}). ^{1}H-NMR ($CDCl_3$, 300 MHz): δ 3.75 (-O-C$\underline{H}_3$, s), 6.52 (H_2, dd, $J1 = 1.80$ y $J2 = 3.41$ Hz), 6.67 (H_{16}, H_{18}, d, $J = 8.40$ Hz), 6.72 (H_3, d, $J = 3.40$ Hz), 7.32 (H_{17}, t, $J = 8.40$ Hz), 7.46-7.57 (H_1, H_6, H_{11}, H_{12}, m), 7.62 (H_5, d, $J = 15.30$ Hz), 8.08 (H_9, H_{10}, d, $J = 8.40$ Hz); ^{13}C-NMR ($CDCl_3$, 75 MHz): δ 55.94 (-O-$\underline{C}H_3$), 104.22 (C_{16}, C_{18}), 112.65 (C_2), 116.00 (C_3), 118.44 (C_6), 119.55 (C_{13}), 127.90 (C_{11}, C_{12}), 129.38 (C_5), 130.35 (C_{17}), 131.39 (C_9, C_{10}), 136.41 (C_{14}), 139.45 (C_8), 144.81 (C_1), 151.86 (C_4), 157.55 (C_{15}, C_{19}), 189.58 (C_7). ESI-MS: *m/z* 335.1285 $[M+H]^+$, Calc. for $C_{21}H_{18}O_4$: 335.1283.

***(2E)-1-{3′,4′-dimethoxy-[1,1′-biphenyl]-4-yl}-3-(furan-2-yl) prop-2-en-1-one (7e)*:** Yield 27%; yellow solid; m.p. 131–134 °C; IR (cm^{-1}): ν_{max} 2951 (-CH_3), 1654 (C = O), 1595 (C = C), 1548 (C = C_{Ar}), 1222 y 1147 (-OCH_3 $_{Ar}$), 1016 (-C-O-C- $_{furane}$), 806 y 754 (C-H_{Ar}). ^{1}H-NMR ($CDCl_3$, 300 MHz): δ 3.94 (-O-C$\underline{H}_3$, s), 3.98 (-O-C$\underline{H}_3$, s), 6.53 (H_2, $s_{apparent}$), 6.74 (H_3, d, $J = 3.30$ Hz), 6.97 (H_{16}, d, $J = 8.40$ Hz), 7.18 (H_5, H_{15}, d, $J = 15.54$ Hz), 7.50 (H_6, d, $J = 15.54$ Hz), 7.55 (H_{19}, s), 7.61 (H_1, s), 7.69 (H_{11}, H_{12}, d, $J = 8.20$ Hz), 8.10 (H_9, H_{10}, d, $J = 8.20$ Hz); ^{13}C-NMR ($CDCl_3$, 75 MHz): δ 56.05 (-O-$\underline{C}H_3$), 110.38 (C_{19}), 111.54 (C_{16}), 112.74 (C_2), 116.30 (C_3), 119.27 (C_6), 119.86 (C_{15}), 126.89 (C_{11}, C_{12}), 129.12 (C_9, C_{10}), 130.59 (C_5), 132.86 (C_{14}), 136.44 (C_{13}), 144.95 (C_8), 145.36 (C_1), 149.34 (C_{18}), 149.43 (C_{17}), 151.76 (C_4), 189.21 (C_7). ESI-MS: *m/z* 335.1277 $[M+H]^+$, Calc. for $C_{21}H_{18}O_4$: 335.1283.

***(2E)-1-{4′-nitro-[1,1′-biphenyl]-4-yl}-3-(furan-2-yl)prop-2-en-1-one (7f)*:** Yield 36%, beige solid; m.p. 183–185 °C; IR (cm^{-1}): ν_{max} 1651 (C = O), 1593 (C = C), 1514 (C = C_{Ar}), 1512 y 1334 (-NO_2), 1006 (-C-O-C- $_{furane}$), 817 y 738 (C-H_{Ar}). ^{1}H-NMR ($CDCl_3$, 300 MHz): δ 6.54 (H_2, dd, $J1 = 1.78$ y $J2 = 3.45$ Hz), 6.76 (H_3, d, $J = 3.45$ Hz), 7.49 (H_6, d, $J = 15.30$ Hz), 7.56 (H_1, d, $J = 1.78$ Hz), 7.64 (H_5, d, $J = 15.30$ Hz), 7.75 (H_{15}, H_{19}, d, $J = 8.60$ Hz), 7.80 (H_{11}, H_{12}, d, $J = 8.90$ Hz), 8.15 (H_{16}, H_{18}, d, $J = 8.60$ Hz), 8.34 (H_9, H_{10}, d, $J = 8.90$ Hz); ^{13}C-NMR ($CDCl_3$, 75,Hz): δ 112.87 (C_2), 116.81 (C_3), 118.91 (C_6), 124.28 (C_{16}, C_{18}), 127.69 (C_{11}, C_{12}), 128.14 (C_{15}, C_{19}), 129.29 (C_9, C_{10}), 131.12 (C_5), 138.23 (C_8), 142.80 (C_{13}), 145.20 (C_1), 146.37 (C_{14}), 147.62 (C_{17}), 151.61 (C_4), 189.04 (C_7). ESI-MS: *m/z* 320.0926 $[M+H]^+$, Calc. for $C_{19}H_{13}NO_4$: 320.0923.

***(2E)-1-{4′-fluoro-[1,1′-biphenyl]-4-yl}-3-(furan-2-yl)prop-2-en-1-one (7g)*:** Yield 38%; beige solid; descomp. p 260 °C; IR (cm^{-1}): ν_{max} 1654 (C = O), 1598 (C = C), 1550 (C = C_{Ar}), 1058 (-C-O-C- $_{furane}$), 813 (C-H_{Ar}). ^{1}H-NMR ($CDCl_3$, 300 MHz): δ 6.53 (H_2, dd, $J1 = 1.80$ y $J2 = 3.36$ Hz), 6.74 (H_3, d, $J = 3.36$ Hz), 7.10–7.22 (H_{16}, H_{18}, m), 7.50 (H_6, d, $J = 15.42$ Hz), 7.54 (H_1, $s_{apparent}$), 7.57–7.64 (H_5, H_{15}, H_{19}, m), 7.67 (H_{11}, H_{12}, d, $J = 8.28$ Hz), 8.11 (H_9, H_{10}, d, $J = 8.28$ Hz); ^{13}C-NMR ($CDCl_3$, 75 MHz): δ 112.79 (C_2), 115.81 (C_{16}), 116.09 (C_{18}), 116.46 (C_3), 119.15 (C_6), 127.16 (C_{11}, C_{12}), 128.93 (C_{15}), 129.04 (C_{19}), 129.15 (C_9, C_{10}), 130.73 (C_5), 136.09, 136.13 (C_{14}), 136.86 (C_8), 144.48 (C_{13}), 145.03 (C_1), 151.72 (C_4), 161.36, 164.65 (C_{17}), 189.20 (C_7). ESI-MS: *m/z* 293.0972 $[M+H]^+$, Calc. for $C_{19}H_{13}FO_2$: 293.0978.

***(2E)-1-([1,1′-biphenyl]-4-yl)-3-(furan-2-yl)prop-2-en-1-one (7h)*:** Yield 65%; yellow solid; m.p. 143–145 °C; IR (cm^{-1}): ν_{max} 1654 (C = O), 1593 (C = C), 1544 (C = C_{Ar}), 1012 (-C-O-C- $_{furane}$), 736 (C-H_{Ar}). ^{1}H NMR ($CDCl_3$, 300 MHz): δ 6.33 (H_2, $s_{apparent}$), 6.74 (H_3, $s_{apparent}$), 7.36–7.63 (H_1, H_5, H_6, H_{15}, H_{17}, H_{19}, m), 7.66 (H_{16}, H_{18}, d, $J = 7.20$ Hz), 7.73 (H_{11}, H_{12}, d, $J = 8.01$ Hz), 8.12 (H_9, H_{10}, d, $J = 8.01$ Hz; ^{13}C NMR ($CDCl_3$, 75 MHz) δ 189.38 (C = O), 151.85 (C_4), 145.63 (C_1), 145.07 (C_{13}), 140.10 (C_{14}), 136.98 (C_8), 130.74 (C_5), 129.19 ($C_{9,10}$), 129.10 ($C_{18,16}$), 128.33 ($C_{16,18}$), 127.42 ($C_{11,12,15,17,19}$), 119.36 (C_6), 116.44 (C_3), 112.85 (C_2); ESI-MS: m/z $[M+H]^+$, 275.1072, Calc. for $C_{19}H_{14}O_2$: 275.1067.

***(2E)-1-(4′-methoxy-[1,1′-biphenyl]-4-yl) -3-(furan-2-yl)prop-2-en-1-one (7i)*:** Yield 85%; yellow solid; descomp. p. 170 °C; IR (cm^{-1}): ν_{max} 1654 (C = O), 1598 (C = C), 1014 (-C-O-C- $_{furane}$), 817 (C-H_{Ar}). ^{1}H NMR ($CDCl_3$, 300 MHz): δ 4.30 (-O-C$\underline{H}_3$, s), 6.99 (H_2, $s_{apparent}$), 7.23 (H_3, $s_{apparent}$), 7.45 (H_{15}, H_{19}, d, $J = 8.30$ Hz), 7.87-8.09 (H_1, H_5, H_6, H_{16}, H_{17}, H_{18}, m), 8.14 (H_{11}, H_{12}, d, $J = 8.01$ Hz), 8.51 (H_9, H_{10}, d, $J = 8.0$ Hz); ^{13}C NMR ($CDCl_3$, 75 MHz) δ: 59.15 (-O-$\underline{C}H_3$), 116.71 (C_2), 118.31 (C_{11}, C_{12}), 120.70 (C_3), 122.95 (C_6), 130.60 (C_9, C_{10}), 132.27 (C_{16}, C_{18}), 133.05 (C_{15}, C_{19}), 134.92 (C_5), 136.12 (C_{14}), 139.92 (C_{13}), 149.27 (C_8), 149.37 (C_1), 155.50 (C_4), 163.87 (C_{17}), 194.19 (C_7); ESI-MS: m/z $[M+H]^+$, 305.1178, Calc. for $C_{20}H_{16}O_3$: 305.1180.

(2E)-1-{6-hydroxy-2′,3′-dimethoxy-[1,1′-biphenyl]-3-yl}-3-(furan-2-yl)prop-2-en-1-one (8a): Yield 61%, beige solid; ^{1}H-NMR ($CDCl_3$, 300 MHz): δ 3.71 (-O-C$\underline{H}_3$, s), 3.95 (-O-C$\underline{H}_3$, s), 6.51 (H_2, dd, $J1 = 1.8$ y $J2 = 3.15$ Hz), 6.71 (H_3, d, $J = 3.15$ Hz), 7.02 (H_{16}, H_{17}, d, $J = 8.11$ Hz), 7.14 (H_{11}, d, $J = 8.50$ Hz), 7.23 (H_{15}, d, $J = 8.11$ Hz), 7.49 (H_1, H_6, d, $J = 15.32$ Hz), 7.62 (H_5, d, $J = 15.32$ Hz), 8.05 (H_9, dd, $J1 = 2.10$ y $J2 = 8.50$ Hz), 8.11 (H_{10}, d, $J = 2.10$ Hz); ^{13}C-NMR ($CDCl_3$, 75 MHz): δ 56.02 (-O-$\underline{C}H_3$), 61.76 (-O-$\underline{C}H_3$), 112.12 (C_{16}), 112.66 (C_2), 115.97 (C_3), 118.40 (C_{11}), 119.18 (C_6), 124.01 (C_{17}), 125.85 (C_{15}), 125.93 (C_8), 130.15 (C_5), 130.41 (C_9), 131.46 (C_{13}), 131.67 (C_{14}), 132.53 (C_{10}), 144.77 (C_1), 145.25 (C_{19}), 151.85 (C_4), 152.82 (C_{18}), 158.24 (C_{12}), 188.16 (C_7). ESI-MS: *m/z* 351.1225 $[M+H]^+$, Calc. for $C_{21}H_{18}O_5$: 351.1232.

***(2E)-1-{6-hydroxy-2′,4′-dimethoxy-[1,1′-biphenyl]-3-yl}-3-(furan-2-yl)prop-2-en-1-one (8b)*:** Yield 45%; yellow oil; ^{1}H-NMR ($CDCl_3$, 300 MHz): δ 3.88 (-O-C$\underline{H}_3$, s), 6.50 (H_2, dd, $J1 = 1.5$ y $J2 = 3.27$ Hz), 6.62 (H_3, d, $J = 3.27$ Hz), 6.68 (H_{16}, H_{18}, dd, $J1 = 2.30$ y $J2 = 8.50$ Hz), 7.08 (H_{11}, d, $J = 8.50$ Hz), 7.30 (H_{15}, d, $J = 8.50$ Hz), 7.48 (H_1, H_5, d, $J = 15.27$ Hz), 7.59 (H_6, d, $J = 15.27$ Hz), 7.97 (H_{10}, d, $J = 2.10$ Hz), 8.01 (H_9, dd, $J1 = 2.10$ y $J2 = 8.50$ Hz); ^{13}C-NMR ($CDCl_3$, 75 MHz): δ 55.62 (-O-$\underline{C}H_3$), 56.21 (-O-$\underline{C}H_3$), 99.24 (C_{18}), 106.33 (C_{16}), 112.63 (C_2), 115.85 (C_{11}), 117.08 (C_3), 118.13 (C_6), 119.30 (C_{13}), 125.98 (C_{10}), 129.96 (C_{15}), 130.01 (C_9), 131.33 (C_5), 132.59 (C_{14}), 133.18 (C_8), 144.70 (C_1), 151.88 (C_4), 156.73 (C_{12}), 158.10 (C_{19}), 161.40 (C_{17}), 188.23 (C_7). ESI-MS: *m/z* 351.1235 $[M+H]^+$, Calc. for $C_{21}H_{18}O_5$: 351.1232.

***(2E)-1-{6-hydroxy-2′,5′-dimethoxy-[1,1′-biphenyl]-3-yl}-3-(furan-2-yl)prop-2-en-1-one (8c)*:** Yield 65%, yellow oil; ^{1}H-NMR ($CDCl_3$, 600 MHz): δ 3.83 (-O-C$\underline{H}_3$, s), 3.85 (-O-C$\underline{H}_3$, s), 6.51 (H_2, dd, $J1 = 1.8$ y $J2 = 3.47$ Hz), 6.70 (H_3, d, $J = 3.47$ Hz), 6.94 (H_{15}, d, $J = 3.05$ Hz), 6.97 (H_{17}, dd, $J1 = 3.05$ y $J2 = 8.90$ Hz), 7.01 (H_{11}, d, $J = 8.90$ Hz), 7.11 (H_{18}, d, $J = 8.90$ Hz), 7.49 (H_5, d, $J = 15.30$ Hz), 7.51 (H_1, d, $J = 1.80$ Hz), 7.60 (H_6, d, $J = 15.30$ Hz), 8.05 (H_9, H_{10}, dd, $J1 = 2.25$ y $J2 = 6.90$ Hz); ^{13}C-NMR ($CDCl_3$, 150 MHz): δ 55.91 (-O-$\underline{C}H_3$), 57.22 (-O-$\underline{C}H_3$), 112.66 (C_{18}), 113.40 (C_2), 114.90 (C_{17}), 116.01 (C_{11}), 117.73 (C_{15}), 117.74 (C_3), 119.14 (C_6), 126.27 (C_{14}), 127.10 (C_{13}), 130.15 (C_{10}), 130.35 (C_9), 131.44 (C_5), 132.46 (C_8), 144.77 (C_1), 149.61 (C_4), 151.80 (C_{12}), 154.82 (C_{19}), 158.16 (C_{16}), 188.16 (C_7). ESI-MS: *m/z* 351.1232 $[M+H]^+$, Calc. for $C_{21}H_{18}O_5$: 351.1232.

***(2E)-1-{6-hydroxy-3′,4′-dimethoxy-[1,1′-biphenyl]-3-yl}-3-(furan-2-yl)prop-2-en-1-one (8e)*:** Yield 64%, yellow solid; m.p. 145-147 °C; IR (cm^{-1}): ν_{max} 3116 (-OH), 2995 (-CH_3), 1645 (C = O), 1600 (C = C), 1556 (C = C_{Ar}), 1271 y 1049 (-$OCH_{3\ Ar}$), 1022 (-C-O-C- $_{furane}$), 813 y 763 (C-H_{Ar}). ^{1}H-NMR ($CDCl_3$, 600 MHz): δ 3.92 (-O-C$\underline{H}_3$, s), 3.94 (-O-C$\underline{H}_3$, s), 6.51 (H_2, dd, $J1 = 1.50$ y $J2 = 3.44$ Hz), 6.70 (H_3, d, $J = 3.44$ Hz), 6.98 (H_{19}, d, $J = 2.02$ Hz), 6.99 (H_{16}, d, $J = 8.20$ Hz), 7.04 (H_9, dd, $J1 = 2.02$ y $J2 = 7.45$ Hz), 7.06–7.10 (H_{15}, m), 7.48 (H_5, d, $J = 15.30$ Hz), 7.51 (H_1, d, $J = 1.50$ Hz), 7.60 (H_6, d, $J = 15.30$ Hz), 7.98–8.01 (H_{10}, H_{11}, m); ^{13}C-NMR ($CDCl_3$, 150 MHz): δ 56.03 (-O-$\underline{C}H_3$), 56.07 (-O-$\underline{C}H_3$), 111.72 (C_{19}), 112.20 (C_{16}), 112.70 (C_2), 115.85 (C_{11}), 116.15 (C_3), 119.01 (C_6), 121.24 (C_{13}), 128.24 (C_{15}), 128.38 (C_{10}), 130.06 (C_5), 130.24 (C_9), 131.12 (C_{14}), 131.25 (C_8), 144.83 (C_1), 149.15 (C_{18}), 149.70 (C_{17}), 151.77 (C_4), 157.07 (C_{12}), 188.24 (C_7). ESI-MS: *m/z* 351.1230 $[M+H]^+$, Calc. for $C_{21}H_{18}O_5$: 351.1232.

***(2E)-1-{6-hydroxy-4′-nitro-[1,1′-biphenyl]-3-yl}-3-(furan-2-yl)prop-2-en-1-one (8f)*:** Yield 31%, yellow solid; m.p. 154-157 °C; IR (cm^{-1}): ν_{max} 3111 (-OH), 1643 (C = O), 1602 (C = C), 1562 (C = C_{Ar}), 1510 y 1346 (-NO_2), 1014 (-C-O-C- $_{furane}$), 850 (C-H_{Ar}). ^{1}H-NMR ($CDCl_3$, 300 MHz): δ 6.59 (H_2, $s_{apparente}$), 6.88 (H_3, d, $J = 3.50$ Hz), 7.06 (H_9, dd, $J1 = 5.76$ y $J2 = 8.45$ Hz), 7.55–7.60 (H_{15}, H_{19}, m), 7.68 (H_1, s), 7.84–7.90 (H_5, H_6, m), 7.99–8.05 (H_{11}, m), 8.08 (H_{10}, d, $J = 5.76$ Hz), 8.25–8.33 (H_{16}, H_{18}, m); ^{13}C-NMR ($CDCl_3$, 75 MHz): δ 112.43 (C_2), 115.86 (C_{11}), 116.08 (C_3), 118.39 (C_6), 122.80 (C_{16}, C_{18}), 126.45 (C_{13}), 129.98 (C_9), 130.06 (C_{15}, C_{19}), 130.17 (C_{10}), 130.82 (C_5), 131.44 (C_{14}), 144.74 (C_8), 145.37 (C_1), 146.78 (C_{17}), 151.73 (C_4), 159.55 (C_{12}), 188.44 (C_7). ESI-MS: *m/z* 336.0872 $[M+H]^+$, Calc. for $C_{19}H_{13}NO_5$: 336.0872.

***(2E)-1-{4′-fluoro-6-hydroxy-[1,1′-biphenyl]-3-yl}-3-(furan-2-yl)prop-2-en-1-one (8g)*:** Yield 54%, yellow solid; m.p. 164–166 °C; IR (cm^{-1}): ν_{max} 3149 (-OH), 1649 (C = O), 1600 (C = C), 1571 (C = C_{Ar}), 1006 (-C-O-C- $_{furane}$), 813 y 744 (C-H_{Ar}). ^{1}H-NMR ($CDCl_3$, 300 MHz): δ 6.48 (H_2, dd, $J1 = 1.70$ y $J2 = 3.20$ Hz), 6.68 (H_3, d, $J = 3.20$ Hz), 6.97 (H_{11}, d, $J = 8.42$ Hz), 7.05–7.17 (H_{16}, H_{18}, m), 7.44 (H_5, d, $J = 15.31$ Hz), 7.48–7.54 (H_1, H_6, H_{19}, m), 7.57 (H_{15}, d, $J = 8.08$ Hz), 7.90 (H_9, dd, $J1 = 2.10$ y $J2 = 8.42$ Hz), 7.95 (H_{10}, d, $J = 2.10$ Hz); ^{13}C-NMR ($CDCl_3$, 75 MHz): δ 112.68 (C_2), 115.16 (C_{11}), 115.44 (C_{16}), 115.97 (C_{18}), 116.18 (C_3), 119.02 (C_6), 127.76 (C_{13}), 129.94 (C_9), 130.25 (C_{15}), 130.98 (C_{19}), 131.09 (C_{10}), 131.87 (C_5), 133.39 (C_8), 133.44 (C_{14}), 144.87 (C_1), 151.73 (C_4), 158.54 (C_{12}), 160.63, 163.90 (C_{17}), 188.67 (C_7). ESI-MS: *m/z* 309.0923 $[M+H]^+$, Calcd for $C_{19}H_{13}FO_3$: 309.0927.

***(2E)-1-(6-hydroxy-[1,1′-biphenyl]-3-yl)-3-(furan-2-yl)prop-2-en-1-one (8h)*:** Yield 66%; orange solid; m.p. 115–118 °C; IR (cm^{-1}): ν_{max} 3429 (-OH), 1710 (C = O), 1647 (C = C), 1600 (C = C_{Ar}), 1006 (-C-O-C- $_{furane}$), 813 y 744 (C-H_{Ar}). ^{1}H-NMR ($CDCl_3$, 300 MHz): δ 6.51 (H_2, dd, $J1 = 3.40$, $J2 = 1.80$ Hz), 6.70 (H_3, d, $J = 3.40$ Hz), 7.13–7.05 (H_{11}, m), 7.56–7.39 (H_{16}, H_{18}, H_5, H_1, H_{19}, H_{15}, H_9, m), 7.61 (H_6, d, $J = 15.30$ Hz), 8.09–7.96 (H_{10}, H_{17}, m); ^{13}C NMR ($CDCl_3$, 75 MHz): δ 112.71 (C_2), 116.16 (C_{16}, C_{18}), 119.07 (C_3), 128.33 (C_6), 128.45 (C_{17}), 129.21 (C_9, C_{10}), 129.36 (C_{15}, C_{19}), 130.26 (C_{11}), 130.34 (C_5), 131.16 (C_{13}), 131.56 (C_8), 136,27 (C_{14}), 144.86 (C_1), 151.79 (C_4), 157.19 (C_{12}), 188.39 (C_7); ESI-MS: *m/z* $[M+H]^+$, 321.1127, Calcd for $C_{19}H_{14}O_3$: 321.1123.

***(2E)-1-(6-hydroxy-4′-methoxy-[1,1′-biphenyl]-3-yl)-3-(furan-2-yl)prop-2-en-1-one (8i)*:** Yield 74%; orange solid; m.p. 144-146 °C; IR (cm^{-1}): ν_{max} 3427 (-OH), 1653 (C = O), 1602 (C = C), 1016 (-C-O-C- $_{furane}$). ^{1}H NMR ($CDCl_3$, 300

MHz): δ 3.86 (-O-C$\underline{H}_3$, s), 6.21 (-OH, s), 6.51 (H_2, dd, J = 3.40, 1.80 Hz), 6.70 (H_3, d, J = 3.40 Hz), 6.99–7.10 (H_{11}, H_{16}, H_{18}, m), 7.43 (H_{15}, H_{19}, d, J = 8.82 Hz), 7.48–7.54 (H_1, H_5, m), 7.60 (H_6, d, J = 15.30 Hz), 8.04–7.94 (H_9, H_{10}, m); ^{13}C NMR ($CDCl_3$, 75 MHz): δ 55.44 (-O-$\underline{C}H_3$), 112.69 (C_2), 114.84 (C_{15}, C_{19}), 115.94 (C_3), 116.08 (C_{11}), 119.12 (C_6), 128.14 (C_9), 128.22 (C_{10}), 129.96 (C_5), 130.26 (C_{14}), 130.40 (C_{16}, C_{18}), 131.16 (C_{13}), 131.46 (C_8), 144.82 (C_1), 151.81 (C_4), 157.18 (C_{17}), 159.67 (C_{12}), 188.38 (C_7); ESI-MS: *m/z* $[M+H]^+$ 291.1021, Calcd for $C_{20}H_{16}O_4$: 291.1017.

Biological activity assays

All compounds were subjected to in vitro evaluation of their cytotoxicity and antitrypanosomal activity against U-937 human macrophages and intracellular amastigotes of *T. cruzi*, respectively.

In vitro cytotoxicity

The cytotoxic activity of the compounds was assessed based on the viability of the human promonocytic cell line U-937 (ATCC CRL-1593.2™) evaluated by the MTT (3-(4,5-dimethylthiazol-2-yl)-2,5-diphenyltetrazolium bromide) assay following the methodology described elsewhere (Taylor et al. 2011). Briefly, U-937 cells grown in tissue flasks were harvested and washed with phosphate buffered saline (PBS) by centrifugation. Cells were counted and adjusted at 1×10^6 cells/mL of RPMI-1640 (Roswell Park Memorial Institute medium-1640) supplemented with 10% fetal bovine serum and 1% of antibiotics (100 U/mL penicillin and 0.1 mg/mL streptomycin) (complete medium). One hundred microlitre of cell suspension were dispensed into each well of a 96-well cell-culture plate and then 100 µL of twofold serial dilutions of the compounds (starting at 200 µg/mL) in complete RPMI 1640 medium were added. Plates were incubated at 37 °C, 5% CO_2 during 72 h in the presence of extracts. The effect of the compounds was determined by adding 10 µL/well of MTT solution (0.5 mg/mL) and incubation at 37 °C for 3 h. The formazan crystals were dissolved by adding 100 µL/well of dimethyl sulfoxide and 30 min incubation. Cell viability was determined according to the intensity of color (absorbance) registered as optical densities (O.D.) obtained at 570 nm in a spectrophotometer (Varioskan™ Flash Multimode Reader—Thermo Scientific, USA). Cells cultured in absence of compounds were used as control of viability (negative control), while benznidazole and doxorrubicin were used as control for noncytotoxic and cytotoxic drugs, respectively. Nonspecific absorbance was corrected by subtracting the O.D. of the blank. Assays were conducted in two independent runs with three replicates per each concentration tested.

In vitro antitrypanosomal activity

T. cruzi, Tulahuen strain transfected with β-galactosidase gene (Buckner et al. 1996) were maintained in vitro as epimastigotes by culturing in modified Novy–MCNeal–Nicolle medium. For the infection of U-937/cells, epimastigotes in early stationary phase of growth (10 days in culture) were harvested, counting in a Neubauer chamber and adjusted at 12.5 parasites/mL of complete RPMI 1640 medium equivalent to 5:1 (parasites per cell) ratio. The U-937 cells were adjusted at 2.5×10^6 cells/mL of complete RPMI-1640 medium containing 0.1 µg/mL of phorbol myristate acetate to induce differentiation to macrophages. Then, 100 µL of this cell suspension were dispensed into each well of a 96-well cell-culture plate. After 24 h of incubation at 37 °C, 5% CO_2, macrophages were infected with stationary growth phase epimastigotes, at the concentration indicated above, and incubated at 34 °C, 5% CO_2 during 24 h to allow the conversion to intracellular amastigotes. Extracelular parasites were removed by washing twice with 100 µL of PBS. Then, 100 µL of each concentration (100 – 25 – 6.12 and 1.56 µg/mL) of compounds were added to infected cells, plates were incubated at 34 °C, 5% CO_2. After 72 h of incubation plate wells were washed twice with PBS and the β-galactosidase activity was measured by spectrophotometry adding 100 µM of the chromogenic substrate CPRG (chlorophenol red-beta-D-galactopyranoside) and 0.1% nonidet P-40 to each well. After 3 h of incubation at 25 °C, absorbance was read at 570 nm in a spectrophotometer (Varioskan™ Flash Multimode Reader—Thermo Scientific, USA). Infected cells exposed to benznidazole were used as control for antitrypanosomal activity (positive control) while infected cells incubated in complete RPMI 1640 culture medium were used as control for infection (negative control). Non-specific absorbance was corrected by subtracting the O.D of the blank. Determinations were done by triplicate in at least two independent experiments (Insuasty et al. 2015).

Statistical analysis

Cytotoxicity was determined according to the percentages of mortality registered to each compound concentration, including benznidazole and complete RPMI 1640 culture medium, calculated by Eq. (1), where the O.D. of control, corresponds to 100% of viability.

$$\%\,\text{Mortality} = 1-[(\text{O.D. exposed cells})/(\text{O.D. control cells})\times 100]. \quad (1)$$

Cytotoxicity was expressed as the half lethal concentrations (LC_{50}) that corresponds to the concentration necessary to eliminate 50% of cells, calculated by Probit analysis

(Finney 1978). In turn, the antitrypanosomal activity was determined according to the percentage of reduction of the amount of parasites obtained for each experimental condition by colorimetry. Parasite reduction was calculated by Eq. (2), where the O.D of control corresponds to 100% of infection.

$$\%\,\text{Parasite reduction} = 1 - [(\text{O.D. exposed parasites})/(\text{O.D. control parasites}) \times 100]. \quad (2)$$

The antitrypanosomal activity was expressed in terms of the EC_{50}, determined by the Probit analysis (Finney 1978). The selectivity index (SI), was calculated by the ratio obtained between the activity observed in cells (LC_{50}) and the activity obtained in parasites (EC_{50}), using the formula:

$$SI = LC_{50}/EC_{50}. \quad (3)$$

In order to compare the different compounds in terms of their biological activity, both cytotoxicity and antitrypanosomal activity were classified as high, moderate, or low, according to the LC_{50} and EC_{50} values. In this way, the cytotoxicity was considered high when the LC_{50} was <100 µM; moderate when the LC_{50} was between 100 and 200 µM and low when the LC_{50} was >200 µM (García et al. 2018). On the other hand, the antitrypanosomal activity was considered high when the EC_{50} was <25 µM, moderate when the EC_{50} was between 25 and 50 µM and low when the EC_{50} was >50 µM (García et al. 2018).

Molecular docking against cruzipain structure

Structures parameterization

To explore the potential mechanism of action of the hybrids, the structure of cruzipain, the major papain-like cysteine protease in *T. cruzi*, was obtained from the Protein Data Bank (Berman et al. 2002). The crystal is in complex with a small molecule that acts as inhibitor of the enzymatic activity (Mott et al. 2009). For our case, we used the characterized binding site of the complex to test the affinity of the hybrids. The structures of the compounds were 3D-modeled using the server Frog2 (Miteva et al. 2010), which implements a force field to obtain by clustering the 3D structures that are most likely to be active, using as input SMILES representations of the molecules. Both, the structures of the selected proteins and the compounds were parameterized using AutoDock Tools (Morris et al. 2009), as proposed in a previous work (Ochoa et al. 2016). In general, hydrogens were added to polar side chains to facilitate the formation of hydrogen bonds, and the Gasteiger partial charges were calculated. Flexibility was included by considering the torsion angles of the structures.

Docking and posterior analysis

The docking search space was delimited with a box containing the binding site identified previously from the crystal. However, the site delimitation was improved with the program Ligsite (Huang and Schroeder 2006), which is useful to detect pockets using geometrical considerations. Subsequently, the docking simulations were carried out with AutoDock Vina (Trott and Olson 2010). The exhaustiveness (internal number of repetitions) was 20 for each protein-compound pair. In addition, five replicas per compound were calculated and averaged to obtain the final docking scores in kcal/mol. The final list was compared against the experimental data using a ranking approach based on the spearman correlation factor. Some of the docked conformations were graphically inspected to check the interactions.

Drug-likeness evaluation

In silico drug-likeness prediction along with further ADMET (absorption, distribution, metabolism, excretion and toxicity) tools presents an array of opportunities which help in accelerating the discovery of new antiparasitic drugs. To find out the drug like properties for all the tested compounds **7a–i** and **8a–i**, the ADMET physicochemical parameters were determined using open-source cheminformatics toolkits such us Molinspiration software (for: MW, H-bond donors, H-bond acceptors, rotatable bonds and topographical polar surface area (PSA) descriptors, ALOGPS 2.1 algorithm from the Virtual Computational Chemistry Laboratory (for: Log $P_{o/w}$ and aqueous solubility LogSw descriptors) and PreADMET 2.0 program to predicted various pharmacokinetic parameters and pharmaceutical relevant properties such as apparent predicted intestinal permeability (App. Caco-2), binding to human serum albumin (Khsa), MDCK cell permeation coefficients and percentage human intestinal absorption (%HIA). These important parameters define absorption, permeability, movement and action of drug molecule. The interpretation of two predicted ADMET properties using the PreADMET program was as shown below:

Value of Caco-2 permeability is classified into three classes:

(1) If permeability < 4, low permeability; (2) if 4 < permeability < 70, medium permeability; and (3) if permeability > 70, higher permeability.

Value of MDCK cell level of permeability can be classified into three classes:

(1) If permeability < 25, low permeability; (2) if 25 < permeability < 500, medium permeability; and (3) if permeability > 500, higher permeability.

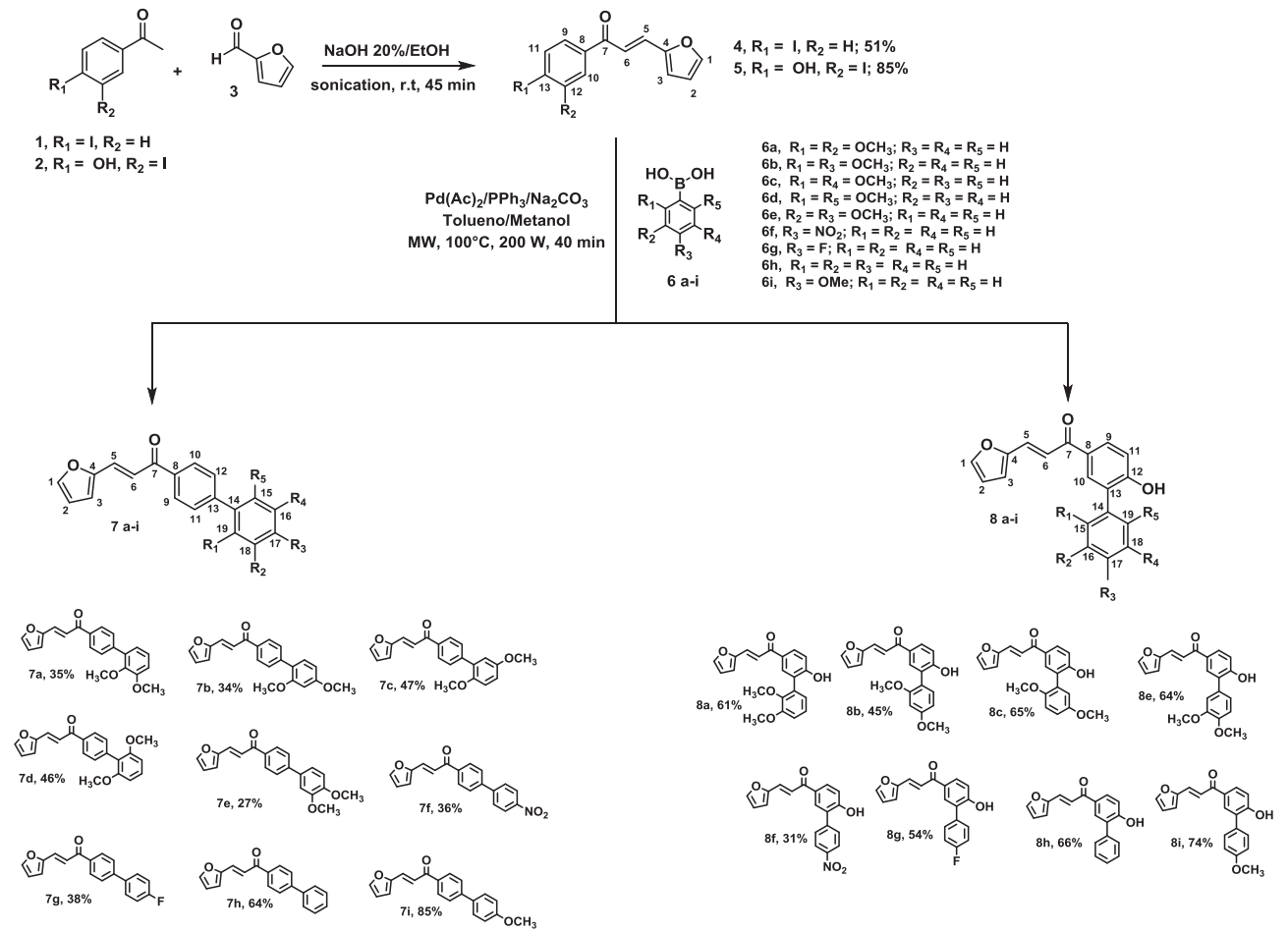

Scheme 1 Synthetic pathway to furanchalcone–biphenyl hybrids

Results and discussion

Chemistry

The synthetic strategy for the preparation of biphenyl-furanchalcones is shown in Scheme 1. Thus, Claisen–Schmidt aldol condensation reaction of acetophenones **1** and **2** with furfural **3**, yielded chalcones **4** and **5** (51% and 85% yield), respectively (Qiao et al. 2012). Microwave assisted Suzuki reaction of furanchalcones **4** and **5** with boronic acids **6a–i** upon (Pierson et al. 2010) afforded arylfuranchalcones **7a–i** and **8a–i** in 17–85%. Compound **8d** could not be obtained under the same reaction conditions.

The structure of each compound was elucidated by a combined study of IR, ESI-MS, ^{1}H NMR, ^{13}C NMR, and bidimensional analysis. The IR spectra exhibit characteristic absorption peaks corresponding to C = O, C = C, C = C_{Ar}, C-O-C, and C-$H_{Ar.}$ ESI-MS spectra exhibit characteristic $[M+H]^{+}$ peaks corresponding to their molecular weights. The assignation of all the signals to individual H or C-atoms was based on typical δ-values and J-constant coupling. ^{1}H-NMR spectrum showed signals around 3.80–3.40 and 7.5 ppm corresponding to -$OCH_{3\ aryl\ group}$, -C = C-H $_{furan\ ring}$ and -CH = C<u>H</u>-C = O, respectively. The ^{13}C-NMR spectra showed signals of C = O (~187 ppm), Ar-O- (~150–153 ppm), furan ring (~144 ppm), -C<u>H</u> = C-C = O (~130 ppm) and –OCH_3 (~56 ppm).

Biological activities

Fourteen of the 17 furanchalcone-biphenyl hybrids synthesized were cytotoxic (with LC_{50} < 100 µM). One of them **7h**, showed moderate cytotoxicity (LC_{50} = 142.75 µM) and two of them, **7f** and **7i**, were noncytotoxic, with LC_{50} values > 200 µM (Table 1).

Dose–response relationship showed that the hybrids **7a–7d**, **8a–8g**, and furanchalcone **4** and **5** were active against

Table 1 In vitro cytotoxicity and antitrypanosomal activity of furanchalcone–biphenyl hybrids

Compound	Cytotoxicity (U-937 cells) LC_{50} [μM]	Antitrypanosomal activity EC_{50} [μM]	IS
7a	16.34 ± 0.12	**17.81 ± 0.75**	0.92
7b	15.82 ± 0.15	**13.59 ± 1.23**	1.16
7c	15.81 ± 0.39	**15.61 ± 1.71**	1.01
7d	16.04 ± 0.26	**15.71 ± 1.86**	1.02
7e	46.27 ± 5.65	83.01 ± 14.23	0.56
7f	393.92 ± 47.07	86.94 ± 6.22	**4.53**
7g	85.68 ± 10.73	99.71 ± 5.76	0.86
7h	142.75 ± 16.95	259.66 ± 48.0	0.55
7i	283.36 ± 102.64	460.0 ± 250.5	0.61
8a	18.99 ± 0.98	**18.15 ± 0.54**	1.05
8b	19.44 ± 1.40	**16.79 ± 2.28**	1.16
8c	15.65 ± 0.17	**15.53 ± 1.85**	1.01
8e	15.61 ± 0.32	**12.59 ± 1.01**	1.24
8f	15.74 ± 0.23	**10.52 ± 0.23**	1.50
8g	17.77 ± 0.46	**13.42 ± 0.39**	1.32
8h	20.56 ± 0.10	64.03 ± 8.37	0.32
8i	17.54 ± 0.22	**30.41 ± 5.46**	0.58
4	24.48 ± 0.98	**15.46 ± 0.19**	1.58
5	17.74 ± 0.72	**13.29 ± 1.04**	1.34
Benznidazole	687.80 ± 16.14	40.3 ± 6.92	17.0

Data represent mean value ± standard deviation in μM. *LC_{50}* lethal concentration 50, *EC_{50}* effective concentration 50, *IS* index of selectivity = LC_{50}/EC_{50}

intracellular amastigotes of *T. cruzi* with EC_{50} values ranging from 10.52 to 30.41 μM. The most active compound was **8f** followed by compounds **8e**, **5**, **8g**, **7b**, **4**, **8c**, **7c**, **7d**, **8b**, **7a**, **8a**, and **8i**. These activities were even higher in comparison to BNZ which displayed an EC_{50} value of 40.3 μM. The remained hybrids **7e**–**7i** and **8h** had low-antitrypanosomal activity with EC_{50} values ranging from 64.03 to 460 μM (Table 1).

Surprisingly, hybrids showed similar range of activities than starting chalcones. This unexpected result could be due to the presence of the Michael acceptor system that is reactive towards nucleophilic amino residues that could be present in target enzymes of *Trypanosoma*, in the same way as described in other parasites (Mottram et al. 2004; Cardona et al. 2014). The IS values calculated for hybrids **7f**, **8e**, **8f**, and **8g** were slightly higher than 1.0 (Table 1). However, the IS could be improved by modifications in the furan ring or by incorporating the active compounds into nanoparticle delivery systems that may reduce the cytotoxicity (Wilczewska et al. 2012). Only compound **7f** showed high IS (4.53). Nevertheless, this compound had not only a very low antitrypanosomal activity but also a low cytotoxicity.

The effect of furanchalcone–biphenyl hybrids was assessed in human cells infected in vitro by *T. cruzi* epimastigotes, a parasite form that is as infective as trypomastigotes and amastigotes (Florencio-Martínez et al. 2010). In addition, the infection using epimastigotes allows the transformation to intracellular amastigotes and their multiplication. The in vitro model of infection used in this work has shown to be adequate to test not only the antiparasitic activity of the new compounds on the parasite form causing the chronic infection but also to evaluate the potential of the compounds to reduce the parasite load inside infected cells (Insuasty et al. 2015).

Based on a structure-activity relationship study, it was noticed that electron withdrawing elements, such as the nitro group or fluorine atom, increased the activity (**7g**, **7f** vs. **7h**, **7i** or **8g**,**8f** vs. **8h**, **8i**). In the monosubstituted compounds series (**7h**, **7i**, **7g**, **7f** vs. **8h**, **8i**, **8g**, **8f**), the presence of the hydroxyl group improved activity. These results agree with other reports for several chalcones, coumarins, cinnamic ester, and triclosan–caffeic acid hybrids (Brenzan et al. 2008; Aponte et al. 2010; Otero et al. 2014; Otero et al. 2017). The effect of the hydroxyl groups may be due to a better molecular recognition ability toward target bioreceptors upon hydrogen bond formation (Patrick 2013). The degree of oxygenation was essential for the activity, with dimethoxylated compounds (**7b**, **7e**, **8b**, and **8e**) exhibiting higher activity than monomethoxylated hybrids (**7i** and **8i**). These results are consistent with a previous report (Otero et al. 2014). Dimethoxylated compounds showed similar activity regardless the position of these oxygenated groups (**7a–7e** and **8a–8e**). This result is inconclusive for these
compounds. However, for the case of cinnamic esters we found that oxygenation in positions 3 and 4 of the phenyl group were fundamental for the activity (Otero et al. 2014), which could be associated with different mechanisms of action.

Docking results

Determining essential genes whose lost is not tolerable by the organism is a potential strategy to identify therapeutic targets in the development of antiparasitic drugs. Cysteine proteases are essential for survival of both *T. cruzi* and *T. brucei* (Otto and Schirmeister 1997; Sajid and McKerrow 2002). Among them, cruzipain has become a relevant protein target to design novel inhibitors for the treatment of Chagas disease (Sajid et al. 2011). This enzyme hydrolyzes chromogenic peptides at the carboxyl terminal of arginine or lysine, and plays a key role in the development and differentiation of the parasite during various life cycle

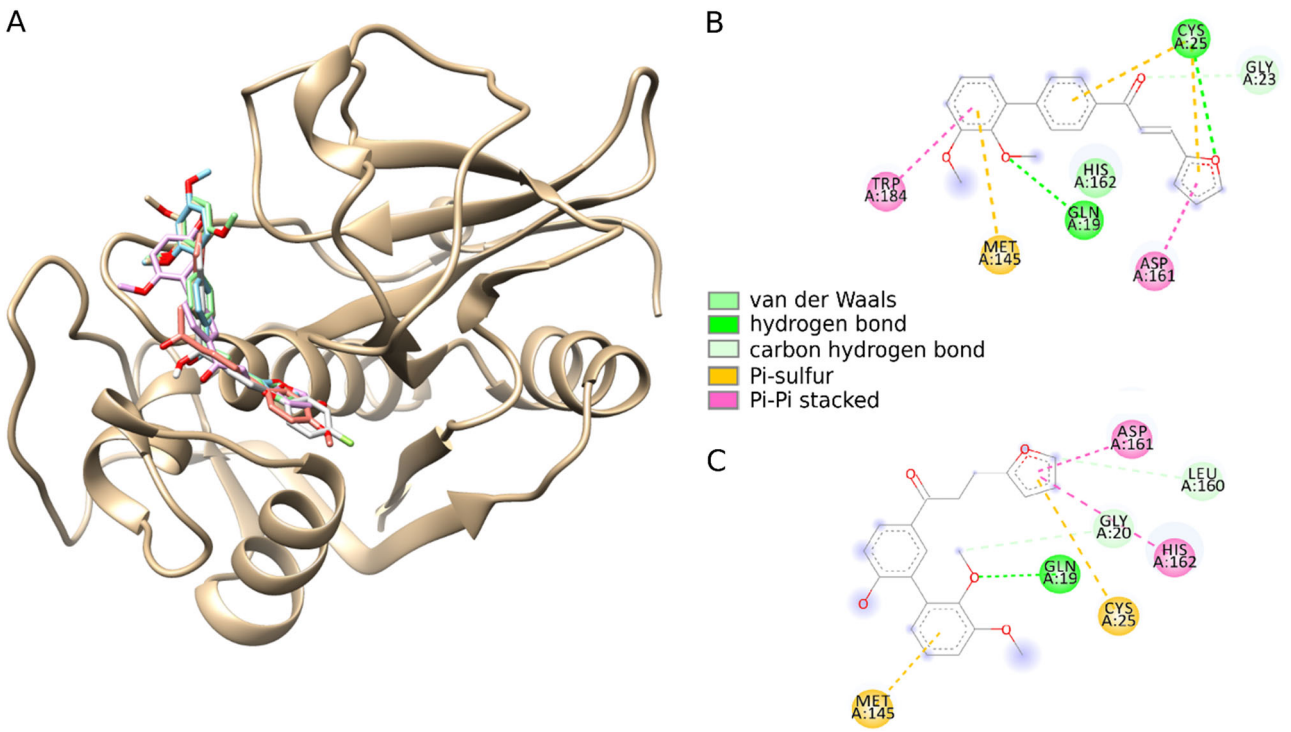

Fig. 4 **a** Interaction of a set of hybrids (seven series) within the delimited active site of *T. cruzi* cruzipain structure (PDB:3I06). **b** 2D representation of interactions formed by compounds **7a** and **7g** with aminoacids of the enzyme

stages (Beaulieu et al. 2010). Chalcones are structurally related to classes of compounds that have been reported as novel potent cruzipain inhibitors, which can effectively cause the death of the parasite (Li et al. 1996; Troeberg et al. 2000; Borchhardt et al. 2010). Therefore, it is of our interest to test in silico the affinity of the designed hybrids and to correlate the results with the experimental findings. Thus, from docking experiments we examined the interactions between the hybrids and key residues of the protein (Fig. 4).

In general, the compounds docked similarly across the delimited binding site, with a set of hydrophobic interactions that potentially confers stability during the binding event. The molecules also form diverse types of interactions, especially π–π and π–sulfur between aromatic amino acids of the protein and ring motifs of the compounds. Table 2 summarizes the average scores per evaluated compound, and the corresponding spearman correlation factor.

According to the ranking correlation (which is higher than 0.5), cruzipain could be a potential candidate of the hybrids evaluated, despite the docking scores being similar within a compound library with small structural differences. However, this initial hint leads us to propose novel experimental evaluations against this molecular target, looking for optimizing the hits obtained in this project in a rational way. These findings are also supported by previous reports of active chalcones against this parasite protein target (Gomes-Vital et al. 2014).

Table 2 Average docking scores per compound evaluated and the spearman correlation against the average experimental binding data

Compound	Average docking score (kcal/mol)
7a	−6.70
7b	−6.94
7c	−6.72
7d	−6.90
7e	−6.64
7f	−6.60
7g	−6.82
7h	−6.74
7i	−6.60
8a	−6.80
8b	−6.70
8c	−6.82
8e	−6.96
8f	−7.10
8g	−6.70
8h	−6.70
8i	−6.80
Spearman correlation	0.608

Drug-likeness prediction studies

We calculated and analyzed various drug-likeness properties for the 17 arylfuranchalcones derivatives. The prediction results are summarized in Table 3. All the compounds showed significant values for the parameters analyzed, exhibiting suitable drug like characteristics. The values were predicted within the range of properties of 95% of currently known drugs. According to Lipinski's rule of five (Lipinski et al. 1997) (an orally active drug has no more than one violation of the criteria) the synthesized compounds **7(a–i)** and **8(a–i)** could be orally active drugs in human. It was observed that all the title compounds exhibited good human intestinal absorption (% HIA) and good percent of human oral absorption (% HOA) ranging from 86 to 100%. Greater HIA and HOA values denote that the synthetized compounds **7(a–i)** and **8(a–i)** could be better absorbed from the intestinal tract upon oral administration.

Among the predicted physico-chemical properties, the molecular PSA is a descriptor that was shown to correlate well with passive molecular transport through membranes and allows the prediction of drug-membrane interactions. A comparison of calculated PSA (Ertl et al. 2000) values for 4-arylfuranchalcones **7** with the 3-arylfuranchalcones **8**, displayed a significant deviation. Thus, when PSA was applied, a correlation between PSA values and EC_{50} numbers showed that a high PSA value (derivatives **8**) favored their anti-trypanosomal activity, whereas low PSA value (compounds **7**) contributed to a reduction of the anti-protozoal activity, suggesting that perhaps these polar compounds tend to have a greater affinity and good ability to penetrate through *T. cruzi*-infected cells. In adittion,

Table 3 In silico ADMET prediction of biphenyl–furanchalcone hybrids

Entry	M.W.[a]	PSA[b](7-200 Å^2)	N_{rot} Bond (<10)	Log Po/w[c] (−2.0 to 6.5)	K_{HSA}[d] (% bound)	Caco-2[e] (nm/s) < 25 poor > 500 great	App. MDCK (nm/s)[f] (<25 poor)	% HIA[g]	Lipinski Rule of five (≤1)	% HOA[h] (>80% is high < 25% is low)
4	324.117	35.460	4	3.509	100	51.521	0.347	100	0	100
5	340.117	57.188	5	2.887	97.80	23.479	0.446	97.01	0	100
7a	334.371	49.623	7	4.580	97.38	57.017	81.856	97.40	0	100
7b	334.371	50.092	7	4.708	98.82	54.934	72.920	97.40	0	100
7c	334.371	51.071	7	4.624	98.48	57.017	11.210	97.40	0	100
7d	334.371	50.849	7	4.588	96.90	57.361	0.396	97.40	0	100
7e	334.371	51.069	7	4.639	98.49	55.190	91.197	97.40	0	100
7f	319.316	80.314	6	3.783	100	6.698	0.357	98.99	0	96
7g	292.309	35.473	5	4.767	100	55.692	37.627	100	0	100
7h	274.318	36.292	5	4.474	100	54.764	81.907	100	0	100
7i	304.345	44.774	6	4.483	100	55.313	17.550	97.98	0	100
8a	350.370	69.510	8	4.042	95.75	46.467	10.145	96.12	0	100
8b	350.370	72.339	8	4.059	97.33	36.032	5.495	96.12	0	100
8c	350.370	70.814	8	4.176	96.94	46.467	0.8118	96.12	0	100
8e	350.370	71.098	8	4.108	95.67	45.840	50.627	96.12	0	100
8f	335.315	100.35	7	4.773	100	16.479	6.561	96.71	0	86
8g	308.308	55.497	6	4.148	100	32.668	27.913	95.84	0	100
8h	290.318	57.639	6	3.937	100	36.692	50.133	95.84	0	100
8i	320.344	66.121	7	3.987	100	35.570	36.004	95.90	0	100

[a]Molecular weight of the molecule

[b]Polar surface area (PSA) (7.0–200.0)

[c]Predicted octanol–water partition coefficient (log $P_{o/w}$)

[d]In vitro binding constant to human serum albumin (K_{HSA})

[e]Predicted human intestinal permeability model (non-active gut-blood barrier transport; <25 poor, >500 great)

[f]Apparent permeability across cellular membranes of Madin–Darby canine kidney (MDCK) cells

[g]Human intestinal absorption (% HIA) (>80% is high, <25% is poor)

[h]Percent of human oral absorption (HOA %)

lipophilicity is an important property for a drug as it influences a number of physiological properties, including transport through lipid bilayers. LogP gives a measure of the lipophilicity of a compound and is a good indicator of permeability across the cell wall (Veber et al. 2002). In this study, all tested compounds exhibited LogP values below 5, ranging from 2.887 to 4.773, suggesting good permeability and permeation across the cell membrane of infected cells. In addition, we calculated the number of rotatable bonds (Nrot), a topological parameter to measure flexibility, and correlated this parameter with the anti-protozoal activity of the tested compounds **7(a–i)** and **8(a–i)**. We found that the most active compounds exhibited an optimum antichagasic activity containing rotatable bonds in the range of 4–8 (see Table 3). This high conformational flexibility of the molecules suggests that all synthesized compounds display good absorption. Moreover, in silico artificial membrane permeation rate across Caco-2 cell monolayers or MDCK cell was calculated for all arylfuranchalcones derivatives. It was found that the passive transmembrane permeation of the novel compounds displayed good permeability values (from 25 to 91 nm/s), except for nitro-substituted arylfuranchalcones **7f** and **8f** which displayed poor cell permeability values (less than 25 nm/s).

Finally, the early prediction of plasma protein binding (K_{HSA}) has vital importance in the characterization of drug distribution in the systemic circulation. Unfavorable log K_{HSA} values can represent a negative effect on clinical development of promising drug candidates for human Chagas disease chemotherapy. Plasma protein binding affinity (K_{HSA}) for the arylfuranchalcones derivatives displayed high binding affinity values (more than 95%). From the therapeutic point of view, the interpretation of predicted ADMET properties showed values very similar for 95% of known drugs (or recommended ranges for an ideal drug) demostrating the potential of the arylfuranchalcones derivatives **7(a–i)** and **8(a–i)** as therapeutic candidates to discover novel drugs for specific treatment of *T. cruzi* infection. These in silico ADMET predictions suggest that arylfuranchalcones derivatives **7(a–i)** and **8(a–i)** follow the criteria for orally active drugs and thus represent a pharmacologically active framework that should be considered in progressing further potential hits.

Conclusions

The synthesis, antitrypanosomal and cytotoxic activities of seventeen furanchalcone derivatives were reported. This study showed that hybrids **7a–7d** and **8a–8g** were active against intracellular amastigotes of *T. cruzi* with EC_{50} of <40 μM. The most active compounds were **7b** and **8e–8g** with an EC_{50} values of 13.59, 12.59, 10.52, and 13.42 μM, respectively. The hybrids **7b–7d** and **8a–8g** exhibited better activity than reference drugs, with compounds **7f**, **8e**, **8f**, and being **8g** the most selective ones. SAR analysis showed that electron withdrawing substituents, such as the nitro group or the fluorine atom, increase the activity. The degree of oxygenation is essential for activity, with dimethoxylated compounds, regardless the position of these oxygenated groups, being more active than monomethoxylated hybrids. In silico ADMET studies of arylfuranchalcones derivatives **7(a–i)** and **8(a–i)**, showed that these novel compounds have good drug like properties, making them promising agents for antichagasic therapy. Physicochemical and ADMET profile of these molecules, such as PSA, LogP and the number of rotatable bonds (Nrot), membrane permeation rate and plasma protein binding (K_{HSA}) showed that these compounds have potential for an eventual development as oral agents and can be significant active drug candidates in search of better and safe antitrypanosomal agents. The structural analysis, allowed us to determine whether cruzipain could be a potential molecular target of the evaluated compounds. Among the cysteine proteases reported in *T. cruzi*, cruzipain is a key protein that has been studied for inhibition purposes with different molecules, including chalcones. In our case, we found a significant prediction correlation with this enzyme, providing us clues for further optimization steps of the synthesized hybrids. This study has showed that these furanchalcone–byphenyl hybrids have potential as candidates for antitrypanosomal drug development.

Acknowledgements The authors thank Universidad de Antioquia (Grants CODI 6203 and CIDEPRO) for financial support.

Compliance with ethical standards

Conflict of interest The authors declare that they have no conflict of interest.

References

Aponte J, Castillo D, Estevez Y, Gonzalez G, Arevalo J, Hammonda G, Sauvain M (2010) In vitro and in vivo anti-Leishmania activity of polysubstituted synthetic chalcones. Bioorg Med Chem Lett 20:100–103

Aponte JC, Verastegui M, Malaga E, Zimic M, Quiliano M, Vaisberg AJ, Gilman RH, Hammond GB (2008) Synthesis, cytotoxicity, and anti-trypanosoma cruzi activity of new chalcones. J Med Chem 51:6230–6234

Beaulieu C, Isabel E, Fortier A, Massé F, Mellon C, Méthot N, Black WC (2010) Identification of potent and reversible cruzipain inhibitors for the treatment of Chagas disease. Bioorg Med Chem Let 20:7444–7449

Berman HM, Battistuz T, Bhat TN, Bluhm WF, Bourne PE, Burkhardt K, Fagan P (2002) The protein data bank. Acta Crystallogr D Biol Crystallogr 58:899–907

Bhambra AS, Ruparelia KC, Tan HL, Tasdemir D, Burrel-Saward H, Yardley V, Beresford KJM, Arroo RRJ (2017) Synthesis and antitrypanosomal activities of novel pyridylchalcones. Eur J Med Chem 128:213–218

Borchhardt DM, Mascarello A, Chiaradia LD, Nunes RJ, Oliva G, Yunes RA, Andricopulo AD (2010) Biochemical evaluation of a series of synthetic chalcone and hydrazide derivatives as novel inhibitors of cruzain from Trypanosoma cruzi. J Braz Chem Soc 21:142–150

Brenzan MA, Vaturu C, Dias B, Ueda T, Young MC (2008) Structure–activity relationship of (−) mammea A/BB derivatives against Leishmania amazonensis. Biomed Pharmacother 62:651–658

Brun R, Bühler Y, Sandmeier U, Kaminsky R, Bacchi CJ, Rattendi D, Lane S, Croft SL, Snowdon D, Yardley V, Caravatti G, Frei J, Stanek J, Mett H (1996) In vitro trypanocidal activities of new *S*-adenosylmethionine decarboxylase inhibitors. Antimicrob Agents Chemother 40:1442–1447

Buckner FS, Verlinde CL, La Flamme AC, Van Voorhis WC (1996) Efficient technique for screening drugs for activity against Trypanosoma cruzi using parasites expressing beta-galactosidase. Antimicrob Agents Chemother 40:2592–2597

Cardona W, Guerra D, Restrepo (2014) A reactivity of δ-substituted α, β-unsaturated cyclic lactones with antileishmanial activity. Mol Simul 40:477–484

Cardona-G W, Yepes AF, Herrera-R A (2018) Hybrid molecules: promising compounds for the development of new treatments against Leishmaniasis and Chagas disease. Curr Med Chem 25:3637–3679

Chen D, Zhang S, Xie L, Xie J, Chen K, Kashiwada Y, Zhou B, Wang P, Cosentino LM, Lee KA (1997) Anti-aids agents—XXVI. Structure–activity correlations of Gomisin-G-related anti-HIV lignans from Kadsura interior and of related synthetic analogues. Bioorg Med Chem 5:1715–1723

Chen M, Zhai L, Christensen SB, Theander TG, Kharazmi A (2001) A Inhibition of fumarate reductase in Leishmania major and L. donovani by chalcones. Antimicrob Agents Chemother 45:2023–2029

Coa JC, Castrillón W, Cardona W, Carda M, Ospina V, Muñoz JA, Vélez ID, Robledo SM (2015) Synthesis, leishmanicidal, trypanocidal and cytotoxic activity of quinoline–hydrazone hybrids. Eur J Med Chem 101:746–753

Coa JC, García E, Carda M, Agut R, Vélez ID, Muñoz JA, Yepes LM, Robledo SM, Cardona WI (2017) Synthesis, leishmanicidal, trypanocidal and cytotoxic activities of quinoline–chalcone and quinoline–chromone hybrids. Med Chem Res 26:1405–1414

De Melo MVP, Abrahim-Vieira BA, Domingos TFS, de Jesus JB, de Sousa ACC, Rodrigues CR, Souza AMT (2018) A comprehensive review of chalcone derivatives as Antileishmanial agents. Eur J Med Chem 150:920–929

Ertl P, Rohde B, Selzer P (2000) Fast calculation of molecular polar surface area as a sum of fragment based contributions and its application to the prediction of drug transport properties. J Med Chem 42:3714–3717

Finney JD (1978) Probit Analysis: Statistical Treatment of the Sigmoid Response Curve, 3rd ed. Cambridge University Press, Cambridge, UK, p 550

Florencio-Martínez L, Márquez-Dueñas C, Ballesteros-Rodea G, Martínez-Calvillo S, Manning-Cela R (2010) Cellular analysis of host cell infection by different developmental stages of *Trypanosoma cruzi*. Exp Parasitol 126:332–336

García E, Coa JC, Otero E, Carda M, Vélez ID, Robledo SM, Cardona WI (2018) Synthesis and antiprotozoal activity of furanchalcone-quinoline, furanchalcone–chromone and furanchalcone–imidazole hybrids. Med Chem Res 27:497–511

Gomes-Vital D, Arribas M, Goulart-Trossini GH (2014) Molecular modeling and docking application to evaluate cruzain inhibitory activity by chalcones and hydrazides. Lett Drug Des Discov 11:249–255

Huang B, Schroeder M (2006) LIGSITE csc: predicting ligand binding sites using the Connolly surface and degree of conservation. BMC Struct Biol 6:19

Insuasty B, Ramirez J, Becerra D, Echeverry C, Quiroga J, Abonia R, Robledo SM, Velez ID, Upegui Y, Muñoz JA, Ospina V, Nogueras M, Cobo J (2015) An efficient synthesis of a new caffeine-based chalcones, pyrazolines and pyrazolo[3-4-b][1-4] diazepines as potential antimalarial, antitrypanosomal and antileishmanial agents. Eur J Chem Med 93:401–413

Ismail MA, Batista-Parra A, Miao Y, Wilson WD, Wenzler T, Brunb R, Boykina DW (2005) Dicationic near-linear biphenyl benzimidazole derivatives as DNA-targeted antiprotozoal agents. Bioorg Med Chem 13:6718–6726

Li R, Chen X, Gong B, Selzer PM, Li Z, Davidson E, Kurzban G, Miller RE, Nuzum EO, McKerrow JH, Fletterick RJ, Gillmor SA, Craik CS, Kuntz ID, Cohen FE, Kenyon GL (1996) Structure-based design of parasitic protease inhibitors. Bioorg Med Chem 4:1421–1427

Lipinski CA, Lombardo F, Dominy BW, Feeney PJ (1997) Experimental and computational approaches to estimate solubility and permeability in drug discovery and development settings. Adv Drug Deliv Rev 23:3–25

Ma L, Chen J, Wang X, Liang X, Luo Y, Zhu W, Wang T, Peng M, Li S, Jie S, Peng A, Wei Y, Chen L (2011) Structural modification of honokiol, a biphenyl occurring in magnolia officinalis: the evaluation of honokiol analogues as inhibitors of angiogenesis and for their cytotoxicity and structure-activity relationship. J Med Chem 54:6469–6481

Meunier B (2008) Hybrid molecules with a dual mode of action: dream or reality? Acc Chem Res 41(69):77

Miteva MA, Guyon F, Tuffïery P (2010) Frog2: Efficient 3D conformation ensemble generator for small compounds. Nucleic Acids Res 38(suppl_2):W622–W627

Morris GM, Huey R, Lindstrom W, Sanner MF, Belew RK, Goodsell DS, Olson AJ (2009) AutoDock4 and AutoDockTools4: (automated docking with selective receptor flexibility. J Comput Chem 30:2785–2791

Mott BT, Ferreira RS, Simeonov A, Jadhav A, Ang KKH, Leister W, McKerrow JH (2009) Identification and optimization of inhibitors of trypanosomal cysteine proteases: cruzain, rhodesain, and TbCatB. J Med Chem 53:52–60

Mottram JC, Coombs GH, Alexander J (2004) Cysteine peptidases as virulence factors of Leishmania. Curr Opin Microbiol 7:375–381

Ochoa R, Watowich SJ, Flórez A, Mesa CV, Robledo SM, Muskus C (2016) Drug search for leishmaniasis: a virtual screening approach by grid computing. J Comput Aided Mol Des 30:541–552

Otero E, Robledo SM, Díaz S, Carda M, Muñoz D, Paños J, Vélez ID, Cardona W (2014) Synthesis and leishmanicidal activity of cinnamic acid esters: structure–activity relationship. Med Chem Res 23:1378–1386

Otero E, García E, Palacios G, Yepes LM, Carda M, Agut R, Vélez ID, Cardona WI, Robledo SM (2017) Triclosan–caffeic acid hybrids: synthesis, leishmanicidal, trypanocidal and cytotoxic activities. Eur J Med Chem 141:73–83

Otto HH, Schirmeister T (1997) Cysteine proteases and their inhibitors. Chem Rev 97:133–172

Patrick GL (2013) An Introduction to Medicinal Chemistry, fifth ed., Oxford University Press, pp. 1-14

Pierson JT, Dumètre A, Hutter S, Delmas F, Laget M, Finet JP, Azas N, Combes S (2010) Synthesis and antiprotozoal activity of 4-arylcoumarins. Eur J Med Chem 45:864–869

Qiao Z, Wang Q, Zhang F, Wang Z, Bowling T, Nare B, Jacobs RT, Zhang J, Ding D, Liu Y, Zhou H (2012) Chalcone–benzoxaborole hybrid molecules as potent antitrypanosomal agents. J Med Chem 55:3553–3557

Sajid M, McKerrow JH (2002) Cysteine proteases of parasitic organisms. Mol Biochem Parasitol 120:1–21

Sajid M, Robertson SA, Brinen LS, McKerrow JH (2011) Cruzain. In: Robinson MW, Dalton JP:Cysteine Proteases of Pathogenic Organisms, Springer, Boston, MA, pp. 100–115

Shaveta, Mishra S, Singh P (2016) Hybrid molecules: the privileged scaffolds for various pharmaceuticals. Eur J Med Chem 124:500–536

Singh P, Anand A, Kumar V (2014) Recent developments in biological activities of chalcones: a mini review. Eur J Med Chem 85:758–777

Taylor VM, Cedeño DL, Muñoz DL, Jones MA, Lash TD, Young AM, Constantino MH, Esposito N, Vélez ID, Robledo SM (2011) In vitro and in vivo studies of the utility of dimethyl and diethyl carbaporphyrin ketals in treatment of cutaneous leishmaniasis. Antimicrob Agents Chemother 55:4755–4764

Troeberg L, Chen X, Flaherty TM, Morty RE, Cheng M, Hua H, Springer C, McKerrow JH, Kenyon GL, Lonsdale-Eccles JD, Coetzer THT, Cohen FE (2000) Chalcone, acyl hydrazide, and related amides kill cultured *Trypanosoma brucei brucei*. Molec Med 6:660–669

Trott O, Olson AJ (2010) AutoDock Vina: improving the speed and accuracy of docking with a new scoring function, efficient optimization, and multithreading. J Comput Chem 31:455–461

Veber DF, Johnson SR, Cheng H-Y, Smith BR, Ward KW, Kopple KD (2002) Molecular properties that influence the oral bioavailability of drug candidates. J Med Chem 45:2615–2623

Vergara S, Carda M, Agut R, Yepes LM, Vélez ID, Robledo S, Cardona W (2017) Synthesis, antiprotozoal activity and cytotoxicity in U-937 macrophages of triclosanhydrazone hybrids. Med Chem Res 26:3262–3273

Wilczewska AZ, Niemirowicz K, Markiewicz KH, Car H (2012) Nanoparticles as drug delivery systems. Pharmacol Rep 64:1020–1037

World Health Organization. Chagas disease (American Trypanosomiasis). http://www.who.int/news-room/fact-sheets/detail/chagas-disease-(american-trypanosomiasis). Accessed 20 Jun 2018

World Health Organization. Neglected tropical diseases. http://www.who.int/neglected_diseases/diseases/en/. Accessed 20 Jun 2018

Zhuang C, Zhang W, Sheng C, Zhang W, Xing C, Miao Z (2017) Chalcone: a privileged structure in medicinal chemistry. Chem Rev 117:7762–7810